HHS Public Access

Author manuscript

Metabolism. Author manuscript; available in PMC 2024 June 14.

Published in final edited form as:

Metabolism. 2024 June ; 155: 155909. doi:10.1016/j.metabol.2024.155909.

Krüppel-like Factor 10 Protects Against Metabolic Dysfunction-Associated Steatohepatitis By Regulating HNF4α-mediated Metabolic Pathways

Xiaoli Pan[1,*], **Shuwei Hu**[1,*], **Yanyong Xu**[1,#], **Raja Gopoju**[1], **Yingdong Zhu**[1], **Fathima N. Cassim Bawa**[1], **Hui Wang**[1], **Jiayou Wang**[1], **Zaid Batayneh**[1], **Alyssa Clark**[1], **Yuhao Zeng**[1], **Li Lin**[2], **Xinwen Wang**[2], **Liya Yin**[1], **Yanqiao Zhang**[1]

[1]Department of Integrative Medical Sciences, Northeast Ohio Medical University, Rootstown, OH 44272, USA

[2]Department of Pharmaceutical Sciences, Northeast Ohio Medical University, Rootstown, OH 44272, USA

Abstract

Background: Krüppel-like factor 10 (KLF10), a zinc finger transcription factor, plays a pivotal role in modulating TGF-β-mediated cellular processes such as growth, apoptosis, and differentiation. Recent studies have implicated KLF10 in regulating lipid metabolism and glucose homeostasis. This study aimed to elucidate the precise role of hepatic KLF10 in developing metabolic dysfunction-associated steatohepatitis (MASH) in diet-induced obese mice.

Methods: We investigated hepatic KLF10 expression under metabolic stress and the effects of overexpression or ablation of hepatic KLF10 on MASH development and lipidemia. We also determined whether hepatocyte nuclear factor 4α (HNF4α) mediated the metabolic effects of KLF10.

Results: Hepatic KLF10 was downregulated in MASH patients and genetically or diet-induced obese mice. AAV8-mediated overexpression of KLF10 in hepatocytes prevented Western diet-induced hypercholesterolemia and steatohepatitis, whereas inactivation of hepatocyte KLF10 aggravated Western diet-induced steatohepatitis. Mechanistically, KLF10 reduced hepatic triglyceride and free fatty acid levels by inducing lipolysis and fatty acid oxidation and inhibiting lipogenesis, and reducing hepatic cholesterol levels by promoting bile acid synthesis. KLF10 highly induced HNF4α expression by directly binding to its promoter. The beneficial effect of

Corresponding author: Dr. Yanqiao Zhang. Department of Integrative Medical Sciences, Northeast Ohio Medical University, 4209 State Route 44, Rootstown, Ohio 44272, USA. yzhang@neomed.edu.

[#]Current address: Key Laboratory of Metabolism and Molecular Medicine of the Ministry of Education, Department of Pathology of School of Basic Medical Sciences, Fudan University, Shanghai, China

[*]Contributed to this work equally

Author contributions

X.P. and Y. Zhang conceived and designed the studies and interpreted the results. Y. Zhang supervised the project. X. Pan, S.H., and Y. Zhang prepared the manuscript. S.H. performed several *in-vivo* and *in-vitro* studies. Y.X., R.G., Y. Zhu., F.N.C.B., H.W., J.W., Z.B., A.C., Y.Z., L.L., X.W. and L.Y. performed various studies. All authors discussed the results and approved the final version of the manuscript.

Disclosure

The authors declare no conflict of interest exists.

KLF10 on MASH development was abolished in mice lacking hepatocyte HNF4α. In addition, the inactivation of KLF10 in hepatic stellate cells exacerbated Western diet-induced liver fibrosis by activating the TGF-β/SMAD2/3 pathway.

Conclusions: Our data collectively suggest that the transcription factor KLF10 plays a hepatoprotective role in MASH development by inducing HNF4α. Targeting hepatic KLF10 may offer a promising strategy for treating MASH.

Keywords

KLF10; HNF4α; MASH; bile acid; cholesterol metabolism

1. Introduction

Metabolic dysfunction-associated steatotic liver disease (MASLD) is characterized by the accumulation of excess fats in the livers of individuals who consume little or no alcohol. This condition spans a spectrum of diseases, ranging from metabolic dysfunction-associated fatty liver (MAFLD) to metabolic dysfunction-associated steatohepatitis (MASH), which may further progress to cirrhosis and liver failure [1]. Currently, MASLD is the most prevalent cause of chronic liver disease, with an estimated overall prevalence of 32.4% worldwide [2]. The prevalence of MASLD is rapidly increasing due to global obesity and type 2 diabetes epidemic. Despite significant progress in understanding the pathogenesis of MASLD, the treatment options for MASH are very limited.

Krüppel-like factor 10 (KLF10) contains a triple C_2H_2 zinc-finger domain and is a DNA-binding transcriptional regulator. It was initially known as transforming growth factor-beta (TGF-β)-inducible early gene 1 (TIEG1) [3]. KLF10 has recently emerged as a potential biomarker for several diseases, including diabetes, cardiac hypertrophy, and osteoporosis [4]. Studies have demonstrated that KLF10 plays a role in regulating lipid metabolism and glucose homeostasis in the liver [5, 6]. Nevertheless, the precise function of KLF10 in the liver and its potential as a therapeutic target for liver diseases have not been elucidated.

In this study, we showed that hepatic KLF10 is reduced in MASH patients and obese mice. Mice lacking *Klf10* in hepatocytes or stellate cells had aggravated MASH or fibrosis development. In contrast, overexpression of hepatic KLF10 prevented the development of MASH in a hepatocyte nuclear factor 4α (HNF4α)-dependent manner. Our data demonstrate that hepatic KLF10 plays a protective role in MASH development.

2. Materials and methods

2.1. Mice, diets, and human tissue

Floxed Klf10 mice on a C57BL/6 background were purchased from GemPharmatech (stock # T018201). C57BL/6J mice (stock # 000664), *ob/ob* mice (stock # 000632), *db/db* mice (stock # 000697), and $Hnf4a^{fl/fl}$ mice (stock # 004665) were purchased from the Jackson Laboratories (Bar Harbor, Maine, USA). $Hnf4a^{fl/fl}$ mice were cross-bred with C57BL/6J mice for at least ten generations [7]. AAV8-TBG-Null or AAV8-TBG-Cre (produced by Vector Biolabs) was injected into $Klf10^{fl/fl}$ or $Hnf4a^{fl/fl}$ mice to generate control

mice (*Klf10*$^{fl/fl}$ or *Hnf4α*$^{fl/fl}$ mice), hepatocyte-specific *Klf10*$^{-/-}$ (*Klf10*$^{Hep-/-}$) mice, or hepatocyte-specific *Hnf4α*$^{-/-}$ (*Hnf4α*$^{Hep-/-}$) mice, respectively. *Klf10*$^{fl/fl}$ mice were cross-bred with Lrat-Cre mice (MMRRC strain # 069595-JAX) to generate control (*Klf10*$^{fl/fl}$) and hepatic stellate cells specific *Klf10* $^{-/-}$ (*Klf10*$^{Hsc-/-}$) mice. All mice were kept in a temperature- and humidity-controlled room with a 12-h light/12-h dark cycle and free access to water and food. The Western diet (WD), which consists of 42% of calories from fat and 0.2% cholesterol, was purchased from Envigo (stock# TD.88137, Indianapolis, IN). The high-fat/cholesterol/fructose (HFCF) diet, comprising 40% of calories from fat, 0.2% cholesterol, and 22% fructose, was purchased from the Research diet (stock # D16051004, New Brunswick, NJ). All mice were randomly assigned to a cage in a blinded manner. Each cage housed ~ 4 mice. The mice were fed a WD or HFCF for up to 20 weeks. Unless otherwise stated, male mice were used and fasted for 5–6 hours before euthanasia. Deidentified human liver samples were obtained from the Liver Tissue Cell Distribution System at the University of Minnesota. All the animal experiments were approved by the Institutional Animal Care and Use Committee at Northeast Ohio Medical University (NEOMED). The use of human tissues was approved by the Institutional Review Board at NEOMED. All research was conducted in accordance with the Declarations of Helsinki and Istanbul.

2.2. Adeno-associated viruses (AAVs)

Human KLF10 coding sequences were cloned into an AAV vector under the control of a mouse albumin promoter to generate AAV8-ALB-hKLF10. AAV8-ALB-Null (control), AAV8-ALB-Cre, and AAV8-ALB-hKLF10 were produced and titrated by Vector BioLabs. Mice were i.v. injected with 2×10^{11} genome copies (GC) of AAVs before feeding with a WD or HFCF diet.

2.3. Plasmid construction, cell culture, and transfection

The promoter sequences of *Hnf4α* were cloned into a pGL3-basic vector (Promega). Mutagenesis was performed using a QuickChange Site-Directed Mutagenesis kit (Agilent), and the mutations were confirmed by sequencing. The mutant sequences (shown in lowercase) in the *Hnf4α* promoter are 5'-GGAAGATTGGTAAGTGACTATTAATGAGCGGGAGGTGGccGccGGGGCAACAGTTGTAATTAGCACCCCAGGTGTCAGTCAGAAAC-3' (−200 bp to −135 bp). HepG2 cells were purchased from ATCC and were free of mycoplasma. Transfection assays were performed using Lipofectamine 3000 (ThermoFisher) [8]. Luciferase activity was determined using Luciferase Assay Systems (cat # E1501, Promega) and normalized to β-galactosidase activity. Primary hepatocytes and primary hepatic stellate cells (HSC) were isolated as described before [9, 10].

2.4. Chemicals

Bovine serum albumin (BSA, cat # A3803), dimethyl sulfoxide (DMSO, cat # D2438), sodium palmitate (cat # P9767), cholesterol (cat # C4951), oleic acid (cat # O3008), and linoleic acid (cat # L9530) were purchased from Sigma. 5-aminoimidazole-4-carboxamideribonucleoside (AICAR, cat # A611700) was purchased from Toronto Research Chemicals Ins.

2.5. mRNA, qPCR, and RNA sequencing

RNA was extracted using Trizol Reagent (Thermo Fisher), and mRNA levels were quantified by quantitative real-time PCR (qRT-PCR) using PowerUP SYBR Green Master Mix (ThermoFisher) on a 7500 Real-Time PCR machine (Applied Biosystems). mRNA levels were normalized to 36B4. Total RNA isolated from livers of mice injected with AAV8-ALB-Null (n=4) or AAV8-ALB-hKLF10 (n=4) was used for cDNA library construction using the standard Illumina procedures. RNA sequencing was conducted using the Illumina NexSeq 500 system [11]. Read sequences were aligned with the whole mouse genome using the Illumina TopHat software and assembled using the Illumina Cufflinks software. KEGG enrichment analysis and volcano plot were performed using the OmicShare tools at www.omicshare.com/tools.

2.6. Plasma biochemistry, FPLC, and biliary bile acid composition

Plasma alanine aminotransferase (ALT) and aspartate aminotransferase (AST) levels were determined using Infinity reagents from Thermo Scientific. Plasma total cholesterol was measured using Infinity reagents (Thermo Scientific). Plasma HDL cholesterol (HDL-C) levels were measured using the HDL-Cholesterol Liquid Reagent (SB-0599–020, Stanbio Laboratory). Total bile acids were measured using a Diazyme Total Bile Acid Test kit (cat # DZ042A-K01, Diazyme laboratories Inc). Plasma LDL cholesterol (LDL-C) levels were measured using a Diazyme LDL-cholesterol assay kit (DZ128A-KY1, Diazyme laboratories Inc). Plasma lipoproteins were separated by Biologic DuoFlow QuadTec 10 System (Bio-Rad) [12], and cholesterol levels were quantified. To analyze hepatic lipid levels, about 100 mg of the liver was homogenized in methanol. Lipids were extracted in chloroform/methanol (2:1 v/v), and hepatic TG or total cholesterol levels were quantified using Infinity reagents (Thermo Scientific). Hepatic free cholesterol (FC) or free fatty acids (FFAs) were determined using kits from Wako Chemical USA (Richmond, VA). Hepatic hydroxyproline level was quantified using a kit from Cell Biolabs (cat # STA675). BA compositions were determined by liquid chromatography–mass spectrometry (LC/MS) [13].

2.7. Western blot assays

Western blot assays were performed using whole liver lysates or microsome extracts of the liver samples as described [11]. The antibody against KLF10 (cat # H00007071-M15) was purchased from Abnova. The antibody against HNF4α (cat # sc-374229) was purchased from Santa Cruz Biotechnology. Antibodies against CYP7A1 (cat # TA351400) or CYP8B1 (cat # TA313734) were purchased from OriGene. Antibodies against LDLR (cat # NBP1–06709), SR-B1 (cat # NB400–101), α-Tubulin (cat # NB100–690) or Calnexin (cat # NB100–1965) were purchased from Novus. Antibodies against phospho-Smad2/3 (cat # 8828) and total Smad2/3 (cat # 5678) were purchased from Cell Signaling Technology. The antibody against α-SMA (cat # ab5694) was purchased from Abcam. Normal rabbit IgG (cat # 12–370) was purchased from EMD Millipore.

2.8. Chromatin immunoprecipitation (ChIP) assay

Livers of mice infected with AAV8-ALB-Null or AAV8-ALB-hKLF10 were homogenized in cold 1xPBS containing the protease inhibitor cocktail (Roche, NJ), 2 μg/ml PMSF, 1

mM EDTA and 1 mM EGTA. Chromatin immunoprecipitation was carried out using a ChIP assay kit (Cat # 17–295; Millipore, MA) with minor modifications according to the manufacturer's protocol [11]. Briefly, the liver homogenate was filtered to remove debris and crosslinked with 1% formaldehyde. After sonication and preclearance with Protein A Agarose/Salmon Sperm DNA, sheared chromatin was immunoprecipitated using an IgG or anti-KLF10 antibody. After elution, the precipitated DNA/antibody complex was digested with proteinase K. DNA was extracted and used for qPCR analysis with primers flanking the KLF10 binding site in the *Hnf4a* promoter. The supernatant before immunoprecipitation of each sample was used as its input control.

2.9. Oil Red O (ORO), hematoxylin and eosin (H&E), or picrosirius red staining

Liver tissues were fixed in 10% formalin and then embedded in OCT or paraffin. The liver sections were stained with ORO, H&E, or picrosirius red. Images were acquired using an Olympus microscope. NAFLD activity score (NAS) was determined after histological grading of steatosis, lobular inflammation, and hepatocyte ballooning, as described [14].

2.10. Immunohistochemical staining

The liver was perfused, fixed in 10% formalin, and embedded in paraffin. Slides were deparaffinized and dehydrated using xylene and a gradient of alcohol. Antigen unmasking was performed using a microwave at high heat for 3 minutes (Cat # H-3300, Vector laboratories). To block endogenous peroxidase activity, sections were incubated in BLOXALL endogenous blocking solution (Cat # SP-6000, Vector Laboratories) for 10 minutes. Sections of the liver were incubated with primary and secondary antibodies following the instructions of the ImmunoCruz rabbit ABC staining system (Cat # sc-2018, Santa Cruz Biotechnology). DAB substrate solution (Cat # SK-4100, Vector Laboratories) was applied to the sections on the slides to visualize the dark brown color.

2.11. Body fat measurement

Body fat was measured using EchoMRI (EchoMRI, LLC, Houston, TX) as described [15], and body fat content was calculated.

2.12. Statistical analysis

All data were expressed as mean±SEM. Statistical significance was analyzed using an unpaired Student *t*-test or ANOVA with a Sidak's multiple comparisons by Prism (GraphPad, CA). Differences were considered statistically significant at $P<0.05$.

3. Results

3.1. Hepatic KLF10 expression is reduced in MASH patients and obese mice

To investigate whether metabolic stress regulated KLF10 expression, we determined hepatic KLF10 expression in MASLD patients and genetically or diet-induced obese mice. In MASH patients, but not patients with simple steatosis (MAFLD), hepatic KLF10 protein levels were significantly reduced by 55% (Figure 1A and 1D). The clinical characteristics of these human subjects is presented in Supplementary Table 1. In murine models of fatty liver

disease induced by high fat/high cholesterol/high fructose (HFCF) diet, Western diet (WD) (Figure 1B) or high fat diet (HFD) (Figure 1C, top panel), hepatic KLF10 protein levels decreased significantly by 74%, 68%, and 52%, respectively (Figure 1B–D). In genetically obese *db/db* or *ob/ob* mice (Figure 1C, bottom panel), hepatic KLF10 protein expression was significantly reduced by 59% and 70%, respectively (Figure 1C–D).

To understand why hepatic KLF10 expression was reduced under metabolic stress conditions, we treated primary hepatocytes with palmitic acid (PA), oleic acid (OA), linoleic acid (LA) or cholesterol (CHO). Treatment with PA, OA or LA, but not CHO, significantly reduced KLF10 protein levels by 62%, 42%, and 50%, respectively (Figure 1E–F), indicating that free fatty acids (FFAs) inhibit KLF10 expression. In contrast, treatment with 5-Aminoimidazole-4-carboxamide ribonucleoside (AICAR), an AMPK activator, significantly induced *Klf10* mRNA expression (Supplementary Figure 1).

To address why hepatic KLF10 expression was significantly reduced in MASH but not MAFLD patients, we analyzed hepatic FFA levels. Interestingly, hepatic FFAs were significantly increased in MASH but not MAFLD patients (Supplementary Figure 2). Given that FFAs markedly inhibits KLF10 expression in primary hepatocytes (Figure 1E–F) and that hepatic FFAs are known to increase in diet-induced or genetic obesity [9, 16], the elevated hepatic FFAs may mediate the significant reduction in hepatic KLF10 expression in MASH or obesity.

3.2. Overexpression of hepatic KLF10 attenuates Western diet-induced MASH and hypercholesterolemia

To start understanding the role of hepatic KLF10 in metabolic homeostasis, we i.v. injected AAV8-ALB-KLF10 or AAV8-ALB-Null (control) into C57BL/6 mice, which were then fed a Western diet for 16 weeks. Overexpression of hepatic KLF10 slightly reduced Western diet-induced gain in body weight and body fat content (Supplementary Figure 3A–B), and resulted in a >33% reduction in plasma ALT and AST levels (Figure 2A; $P<0.05$) as well as a 28.2% reduction in plasma total cholesterol (TC) (Figure 2B; $P<0.01$) and a 43% reduction in plasma LDL-C levels (Figure 2C; $P<0.05$) with no change in plasma HDL-C levels (Supplementary Figure 3C). Analysis of the lipoprotein profile by fast protein liquid chromatography (FPLC) showed that hepatic KLF10 overexpression reduced plasma LDL-C levels (Figure 2D).

In the liver, hepatic KLF10 overexpression significantly reduced the liver-to-body weight ratio (Supplementary Figure 3D) as well as hepatic triglyceride (TG) and free fatty acid (FFA) levels (Figure 2E–F; $P<0.05$). Overexpression of hepatic KLF10 also reduced hepatic TC and free cholesterol (FC) by 32% and 54%, respectively (Figure 2G–H; $P<0.01$), which were further confirmed by histological staining with hematoxylin/eosin (H&E) or oil red O (ORO) (Figure 2I). Consistent with these findings, overexpression of hepatic KLF10 also significantly reduced the histological grading of steatosis, lobular inflammation, and hepatocyte ballooning, and the NAFLD activity score (NAS) by 27% (Figure 2J; $P<0.01$). Thus, overexpression of hepatic KLF10 protects against Western diet-induced MASH and hypercholesterolemia.

Fructose is known to promote the development of steatohepatitis by promoting de novo lipogenesis (DNL) and reactive oxygen species (ROS) production [17]. When C57BL/6 mice were fed a high fat/cholesterol/fructose (HFCF) diet, hepatic overexpression of KLF10 significantly reduced plasma ALT and AST levels by 55% and 45%, respectively (Supplementary Figure 4A), and also significantly reduced hepatic levels of TG, TC, FC, and hydroxyproline by 18%, 38%, 52%, and 27%, respectively (Supplementary Figure 4B–E), which were further corroborated by histological staining with H&E, ORO and picrosirius red (Supplementary Figure 4F). Hepatic KLF10 overexpression significantly reduced HFCF diet-induced NAS by 38% and fibrosis score by 31% (Supplementary Figure 4G). Together, the data of Figure 2 and supplementary Fig. 4 demonstrate that hepatic KLF10 overexpression is sufficient to protect against diet-induced MASH.

3.3. Ablation of hepatocyte KLF10 aggravates Western diet-induced steatohepatitis and hypercholesterolemia

To investigate whether the loss of hepatocyte KLF10 regulated the pathogenesis of MASH, we generated hepatocyte-specific *Klf10*$^{-/-}$ (*Klf10*$^{Hep-/-}$) mice by i.v. injection of AAV8-TBG-Cre into *Klf10*$^{fl/fl}$ mice. *Klf10*$^{Hep-/-}$ mice and their control mice (i.e., *Klf10*$^{fl/fl}$ mice injected i.v. with AAV8-TBG-Null) were then fed a Western diet for 16 weeks. Hepatocyte-specific knockdown of *Klf10* did not affect body weight or body fat content (Supplementary Figure 5A–B), but significantly raised plasma ALT and AST levels (Figure 3A; $P<0.05$). Loss of hepatocyte *Klf10* also increased plasma total cholesterol by 39% (Figure 3B; $P<0.01$) and LDL-C by 49% (Figure 3C; $P<0.01$), with a trend of inducing plasma HDL-C levels (Supplementary Figure 5C). The changes in plasma cholesterol levels were also confirmed by fast protein liquid chromatography (FPLC) (Figure 3D).

In the liver, the loss of hepatocyte *Klf10* significantly increased the liver-to-body weight ratio (Figure 3E) and significantly raised hepatic total cholesterol (TC) by 20% (Figure 3F) and free cholesterol (FC) by 33% (Figure 3G). H&E and oil red O staining confirmed more lipid accumulation in *Klf10*$^{Hep-/-}$ mice (Figure 3H). In addition, histological grading studies showed that *Klf10*$^{Hep-/-}$ mice had more steatosis, lobular inflammation, and hepatocyte ballooning and increased NAFLD activity score (NAS) by 60% (Figure 3I). Together, the data of Figure 3 demonstrate that hepatocyte KLF10 is required for protection against Western diet-induced MASH and hypercholesterolemia.

3.4. Hepatocyte KLF10 coordinates the regulation of genes contributing to steatohepatitis

Our gain- and loss-of-function studies have demonstrated that hepatocyte KLF10 protects against diet-induced MASH. To determine the underlying mechanisms, we performed RNA-Seq using liver samples isolated from mice infected with AAV8-ALB-Null or AAV8-ALB-KLF10. This analysis identified 5,593 differentially expressed genes (DEGs), comprising 3,458 down-regulated genes and 2,135 up-regulated genes. KEGG pathway enrichment analysis revealed that these DEGs were predominantly enriched in metabolic pathways, particularly those related to cholesterol and bile acid metabolism, TGF-β signaling pathway, etc. (Supplementary Figure 6A). Some of the top up-regulated genes (e.g., *Ces1g/Ces1*, *Cyp7a1*, *Akr1d1*) and down-regulated genes (e.g., *Pcsk9*, *Timp1*, *Col5a2*) are presented in

supplementary Figure 6B. Carboxylesterase (CES) *1g Ces1g/Ces1* has triglyceride hydrolase (TGH) activity and protects against hepatic steatosis [12]. Cholesterol 7α-hydroxylase (CYP7A1) is the rate-limiting enzyme of bile acid (BA) synthesis in the classic pathway. Aldo-keto reductase family 1 member D1 (AKR1D1) also promotes BA synthesis [18]. Proprotein convertase subtilisin/kexin type 9 (PCSK9) binds to LDL receptor (LDLR) and targets it for lysosomal degradation [19]. Tissue inhibitor of metalloproteinase 1 (TIMP1) and collagen type 5 α2 (COL5A2) play a role in fibrogenesis. Therefore, we determined the expression of genes involved in *de novo* lipogenesis (DNL), fatty acid oxidation (FAO), lipolysis, BA synthesis, cholesterol uptake, cholesterol excretion, inflammation, and fibrogenesis.

In mice overexpressing hepatocyte KLF10, genes involved in fatty acid synthesis, including acetyl-CoA carboxylase 2 (*Acc2*), fatty acid synthase (*Fasn*), elongation of long-chain fatty acid family 6 (*Elovl6*), were significantly reduced whereas genes involved in lipolysis, including *Ces1d* [20], *Ces1g/Ces1* [12, 21], *Ces2c/Ces2* [22], or FAO, including peroxisome proliferation-activated receptor α (*Pparα*), carnitine palmitoyltransferase 1a (*Cpt1a*), *Cpt1b*, *Cpt2*, were significantly induced (Figure 4A). These changes may account for the reduced hepatic TG and FFA levels (Figure 2E–F). Overexpression of hepatocyte KLF10 also significantly induced hepatic mRNA levels of genes involved in BA synthesis, including *Cyp7a1*, sterol 12α-hydroxylase (*Cyp8b1*), *Akr1d1*, hepatocyte nuclear factor 4α (*Hnf4α*), and cholesterol excretion, including ATP binding cassette group G member 8 (*Abcg8*), and significantly inhibited *Pcsk9* expression (Figure 4B). The significant induction of BA synthetic genes and ABCG8 and the significant inhibition of PCSK9 may account for the reduced hepatic TC and FC levels (Figure 2G–H) and plasma LDL-C levels (Figure 2B–D), respectively. In addition, hepatic overexpression of KLF10 significantly inhibited genes involved in inflammation, including tumor necrosis factor α (*Tnfα*), interleukin 6 (*Il6*), *Il1β*, or fibrogenesis, including *Col1a1*, *Col1a2*, alpha-smooth muscle actin (*αSma*). These latter changes were consistent with the finding that hepatic KLF10 overexpression reduces liver injury and NAS (Figure 2).

Consistent with the changes in mRNA levels, hepatic KLF10 overexpression significantly induced hepatic protein levels of KLF10, CYP7A1, CYP8B1, LDLR, and HNF4α by 2.6, 2.2, 2.8, 5, and 2.7 fold, respectively (Figure 4D–E). The high induction of LDLR protein levels may be due to the inhibition of PCSK9 (Figure 4B). Consistent with the induction of CYP7A1, hepatic overexpression of KLF10 increased biliary taura-chenodeoxycholic acid (T-CDCA), taura-ursodeoxycholic acid (T-UDCA), and taura-lithocholic acid (TCA) levels by 1.9, 2.1, and 2.0 fold, respectively (Figure 4F).

In line with the gain of function study, the loss of hepatocyte *Klf10* significantly induced DNL lipogenic genes (*Acc1*, *Acc2*, *Fasn, Elovl6*) and significantly inhibited *Ces1g/Ces1* (Figure 4G). Hepatocyte KLF10 deficiency also significantly reduced hepatic mRNA levels of *Klf10*, *Cyp7a1*, *Cyp8b1*, *Akr1d1*, *Scarb1*, *Ldlr*, *Hnf4α*, *Abcg5* and *Abcg8* (Figure 4H), and significantly induced mRNA levels of *Il1β*, *Timp1*, *Col1a1*, *Col1a2*, and *αSma* (Figure 4I). Consistent with the changes in mRNA levels, the loss of hepatocyte *Klf10* significantly decreased hepatic protein levels of KLF10, CYP7A1, CYP8B1, SR-BI, LDLR, and HNF4α

by 55%, 44%, 48%, 35%, 63% and 65%, respectively (Figure 4J–K). Thus, the loss of function studies support the findings observed from the gain of function studies.

3.5. Hepatocyte KLF10 prevents MASH development via HNF4α

The data of Figures 2–4 show that hepatocyte KLF10 prevents MASH likely by inhibiting genes involved in DNL, inflammation, and fibrogenesis, and inducing genes involved in lipolysis, FAO, and bile acid synthesis. Interestingly, hepatocyte HNF4α has similar functions [7, 23]. Overexpression of hepatic KLF10 significantly induces HNF4α by 2.7 fold whereas loss of hepatocyte KLF10 significantly inhibits HNF4α by 65% (Figure 4). Thus, we asked whether hepatocyte KLF10 protected against MASH via induction of hepatocyte HNF4α.

We i.v. injected AAV8-ALB-Null or AAV8-ALB-hKLF10 into hepatocyte-specific *Hnf4a*$^{-/-}$ (*Hnf4a*$^{Hep-/-}$) mice or *Hnf4a*$^{fl/fl}$ mice, and then fed these mice a Western diet for 16 weeks. Hepatic KLF10 overexpression significantly reduced body weight at 8 weeks and 12 weeks (Figure 5A). As expected, overexpression of hepatocyte KLF10 in *Hnf4a*$^{fl/fl}$ mice significantly reduced plasma ALT and AST levels (Figure 5B–C), as well as hepatic levels of TG (Figure 5D), FFA (Figure 5E), TC (Figure 5F), FC (Figure 5G) and hydroxyproline (Figure 5H), and significantly raised hepatic BA levels (Figure 5I). Interestingly, all these changes were abolished in *Hnf4a*$^{Hep-/-}$ mice (Figure 5B–I), suggesting that the metabolic effects of KLF10 are dependent on HNF4α.

At the gene expression levels, overexpression of hepatic KLF10 (Figure 5J) significantly reduced hepatic lipogenic genes (*Acc1*, *Elovl6*) and inflammatory/fibrogenic genes (*Tnfa*, *Il1β*, *αSma*), and significantly induced lipolytic and FAO genes (*Ces1d*, *Ces1g*, *Ces2c*, *Cpt1a*, *Cpt1b*, *Cpt2*), BA synthetic genes (*Cyp7a1*, *Cyp8b1*), and cholesterol excretion genes (*Abcg5*, *Abcg8*) in *Hnf4a*$^{fl/fl}$ mice, but not in *Hnf4a*$^{Hep-/-}$ mice (Figure 5K). Thus, the changes in gene expression are consistent with the phenotypic changes. Interestingly, hepatic KLF10 expression was significantly reduced by 70% in *Hnf4a*$^{Hep-/-}$ versus *Hnf4a*$^{fl/fl}$ mice infected with AAV8-ALB-Null (Figure 5J) suggesting that HNF4α is a positive regulator of hepatic KLF10 expression. Taken together, the data of Figure 5 demonstrate that overexpression of hepatocyte KLF10 protects against MASH development via the induction of HNF4α.

3.6. HNF4α is a direct target of KLF10

The data of Figure 5 demonstrate that hepatocyte HNF4α mediates the protective effect of KLF10 on MASH. Next, we investigated how KLF10 regulated HNF4α expression. Transfection of HepG2 cells with an expression plasmid expressing KLF10 significantly induced the −1.0 kb and −0.3 kb *Hnf4a* promoter activities by >3.7 fold (Figure 6A–B). Such an induction was completely abolished when a KLF10 binding site at between −184 bp and −177 bp was mutated (Figure 6C). The chromatin immunoprecipitation (ChIP) assay utilizing liver tissues demonstrated that KLF10 protein bound to the same region of the *Hnf4a* promoter (Figure 6D; $P<0.01$). Together, the data of Figure 6 indicate that HNF4α is a direct target of KLF10.

3.7. Hepatic stellate cell-specific deletion of KLF10 exacerbates liver fibrosis

Hepatic stellate cells (HSC) play a key role in liver fibrogenesis in response to liver injury, TGFβ, inflammation, etc. [24]. Since liver fibrosis is an important component of MASH development, we investigated whether KLF10 in HSC regulated liver fibrosis. We generated HSC-specific *Klf10*$^{-/-}$ (*Klf10*$^{Hsc-/-}$) mice by crossbreeding *Klf10*$^{fl/fl}$ mice with *Lrat-Cre* mice. *KLF10*$^{fl/fl}$ mice and *Klf10*$^{Hsc-/-}$ mice were then subjected to a high fat/cholesterol/fructose (HFCF) diet for 20 weeks. Loss of HSC *Klf10* tended to increase plasma ALT levels (P=0.07) and AST levels (P=0.05) (Figure 7A), but significantly increased hepatic hydroxyproline levels by 3.6 fold. (Figure 7B), which was further confirmed by picrosirius red staining of liver sections (Figure 7C). Immunohistochemical staining showed increased αSMA protein expression in the liver (Figure 7D).

Klf10$^{Hsc-/-}$ mice had significantly reduced hepatic *Klf10* mRNA and protein levels (Figure 7E–G). *Klf10*$^{Hsc-/-}$ mice also had significantly increased hepatic *Tgfβ*, *Timp1*, *Timp2*, *αSma*, *Col1a1*, and *Col4a1* mRNA levels and significantly reduced hepatic *Hnf4α* mRNA levels (Figure 7E). Furthermore, the loss of HSC *Klf10* significantly raised hepatic phosphorylated SMAD2/3 protein levels by 2.5 fold and αSMA protein levels by 2.9 fold whereas hepatic HNF4α protein levels tended to decrease (Figure 7F–G).

To further understand how the loss of KLF10 in HSC regulated fibrogenesis, we isolated HSC from *Klf10*$^{fl/fl}$ mice and *Klf10*$^{Hsc-/-}$ mice and used the culture media to treat primary hepatocytes isolated from C57BL/6 mice. Interestingly, treatment with the conditioned media of HSC lacking *Klf10* significantly reduced *Hnf4α* mRNA levels and significantly induced mRNA levels of *Timp1*, *Mcp1*, and *Il1β* in wild-type primary hepatocytes (Figure 7H). In primary hepatocytes isolated from *Klf10*$^{Hsc-/-}$ mice, *Hnf4α* mRNA and protein levels were also significantly reduced (Figure 7I–J), suggesting a crosstalk between HSC and hepatocytes. Interestingly, we found that *Hnf4α* was expressed at a low level in HSC (Supplementary Figure 7A). Furthermore, *Hnf4α* was significantly reduced whereas *Tgfβ* and *αSma* were significantly induced in HSC isolated from *Klf10*$^{Hsc-/-}$ mice (Supplementary Figure 7B). Thus, the data of Figure 7H–J and Supplementary Figure 7 suggest that the loss of KLF10 in HSC promotes fibrogenesis likely activation of hepatocyte and/or direct activation of HSC, and the inhibition of HNF4α may play a role in this process. Taken together, our data indicate that the ablation of KLF10 in HSC activates the TGFβ-SMAD2/3 pathway likely via interaction with hepatocytes or self-activation, leading to increased fibrogenesis.

4. Discussion

When fed a methionine and choline deficient diet (MCDD), global *Klf10*$^{-/-}$ mice develop enhanced liver injury and apoptosis [25]. In a separate study, Lee *et al.* showed global *Klf10*$^{-/-}$ mice exhibited severe liver steatosis, inflammation, and fibrosis when fed a high sucrose diet [26]. These studies illustrate the protective role of KLF10 in liver injury. In this work, we show that overexpression of hepatocyte KLF10 protects against Western diet-induced MASH whereas loss of hepatocyte KLF10 has opposite effects. Thus, the loss of hepatocyte KLF10 is likely responsible for the phenotypes displayed in global *Klf10*$^{-/-}$ mice. Interestingly, Yang *et al.* showed that AAV-mediated overexpression of

KLF10 promotes MASH development [27]. In the latter study conducted by Yang *et al.*, the expression of KLF10 was not controlled by a liver or hepatocyte-specific promoter, and less animals were used per group (n=5) [27]. In contrast, we used the albumin promoter to drive KLF10 overexpression in the liver and used more animals per group. Importantly, our data from the gain of function studies were reproducible when two different diets (WD and HFCF diets) were used, and they were also supported by the loss of function studies in which hepatocyte-specific *Klf10*$^{-/-}$ mice were used. Nonetheless, we are unsure if the microbiota in different animal facilities contributed to the different observations.

Using gain and loss of function approaches, we demonstrate that hepatocyte KLF10 protects against MASH development by induction of hepatic HNF4α. Indeed, KLF10 and HNF4α share some common biological functions, such as induction of lipolysis, FAO, and BA synthesis from cholesterol [7]. By reducing hepatic FFA and FC levels, KLF10 decreases hepatic lipotoxicity. Since lipotoxicity plays a key in the progression of MASLD to MASH [28, 29], KLF10 may prevent MASH development by reducing hepatic lipotoxicity via HNF4α.

KLF10 is an early TGFβ-inducible gene, but its *in vivo* role in HSC activation has not been investigated before. By using HSC-specific *Klf10*$^{-/-}$ mice, we show that KLF10 in HSC is important for preventing HFCF diet-induced stellate activate activation and fibrogenesis. In the co-culture study, the loss of *Klf10* in HSC causes a reduction in HNF4α and an induction of proinflammatory and fibrogenic genes in hepatocytes, which may in turn lead to activation of HSC. Unexpectedly, our studies also show that HNF4α is expressed at a low level in HSC, and is reduced in HSC lacking *Klf10*. It will be intriguing to investigate whether the loss of HNF4α in HSC promotes fibrogenesis. In isolated HSC lacking *Klf10*, both TGFβ and αSMA are highly induced, suggesting that the loss of KLF10 in HSC may directly promote HSC activation. Thus, the loss of KLF10 in HSC causes fibrogenesis likely via activation of hepatocytes and/or direct activation of HSC, and the inhibition of HNF4α may mediate these processes.

In MASLD patients, hepatic KLF10 expression is reduced in MASH but not in MAFLD patients, which likely results from the elevated FFAs in the liver of MASH patients, as our data show that FFAs inhibit KLF10 expression in primary hepatocytes. In diet-induced or genetic obesity, hepatic FFAs are known to be induced [9, 16]. Indeed, hepatic KLF10 expression is significantly reduced to a similar extent in these mice. Previous studies show that FFAs inhibit HNF4α expression [30]. Our data show that KLF10 expression is significantly reduced in *Hnf4α*$^{Hep-/-}$ mice. Thus, hepatic KLF10 expression is reduced in MASH or obesity likely via an FFA-HNF4α pathway.

In summary, we have shown that hepatic KLF10 is downregulated in MASH and obesity. The downregulation of hepatic KLF10 may play an important role in the pathogenesis of MASH development under metabolic stress. In addition, we demonstrate that hepatocyte KLF10 plays a pivotal role in protection against MASH development through the modulation of HNF4α, and that KLF10 in HSC protects against fibrogenesis likely via the inhibition of hepatocyte activation or direct inhibition of HSC activation. Furthermore,

hepatic KLF10 prevents Western diet-induced hypercholesterolemia. Thus, targeting hepatic KLF10 may offer a new avenue for therapeutic interventions of MASLD.

Supplementary Material

Refer to Web version on PubMed Central for supplementary material.

Acknowledgements

The work was supported in part by NIH grant R01HL142086.

Data available

All data are available upon request.

References

[1]. Hutchison AL, Tavaglione F, Romeo S, Charlton M. Endocrine aspects of metabolic dysfunction associated steatotic liver disease (MASLD): Beyond insulin resistance. J Hepatol. 2023.

[2]. Riazi K, Azhari H, Charette JH, Underwood FE, King JA, Afshar EE, et al. The prevalence and incidence of NAFLD worldwide: a systematic review and meta-analysis. Lancet Gastroenterol Hepatol. 2022;7:851–61. [PubMed: 35798021]

[3]. Subramaniam M, Hawse JR, Rajamannan NM, Ingle JN, Spelsberg TC. Functional role of KLF10 in multiple disease processes. Biofactors. 2010;36:8–18. [PubMed: 20087894]

[4]. Memon A, Lee WK. KLF10 as a Tumor Suppressor Gene and Its TGF-beta Signaling. Cancers (Basel). 2018;10.

[5]. Ruberto AA, Grechez-Cassiau A, Guerin S, Martin L, Revel JS, Mehiri M, et al. KLF10 integrates circadian timing and sugar signaling to coordinate hepatic metabolism. Elife. 2021;10.

[6]. Yang X, Chen Q, Sun L, Zhang H, Yao L, Cui X, et al. KLF10 transcription factor regulates hepatic glucose metabolism in mice. Diabetologia. 2017;60:2443–52. [PubMed: 28836014]

[7]. Xu Y, Zhu Y, Hu S, Xu Y, Stroup D, Pan X, et al. Hepatocyte Nuclear Factor 4alpha Prevents the Steatosis-to-NASH Progression by Regulating p53 and Bile Acid Signaling (in mice). Hepatology. 2021;73:2251–65. [PubMed: 33098092]

[8]. Kijima T, Eguchi T, Neckers L, Prince TL. Monitoring of the Heat Shock Response with a Real-Time Luciferase Reporter. Methods Mol Biol. 2018;1709:35–45. [PubMed: 29177649]

[9]. Xu Y, Hu S, Jadhav K, Zhu Y, Pan X, Bawa FC, et al. Hepatocytic Activating Transcription Factor 3 Protects Against Steatohepatitis via Hepatocyte Nuclear Factor 4alpha. Diabetes. 2021;70:2506–17. [PubMed: 34475098]

[10]. Mederacke I, Dapito DH, Affo S, Uchinami H, Schwabe RF. High-yield and high-purity isolation of hepatic stellate cells from normal and fibrotic mouse livers. Nat Protoc. 2015;10:305–15. [PubMed: 25612230]

[11]. Xu Y, Li Y, Jadhav K, Pan X, Zhu Y, Hu S, et al. Hepatocyte ATF3 protects against atherosclerosis by regulating HDL and bile acid metabolism. Nat Metab. 2021;3:59–74. [PubMed: 33462514]

[12]. Xu J, Li Y, Chen WD, Xu Y, Yin L, Ge X, et al. Hepatic carboxylesterase 1 is essential for both normal and farnesoid X receptor-controlled lipid homeostasis. Hepatology. 2014;59:1761–71. [PubMed: 24038130]

[13]. Alnouti Y, Csanaky IL, Klaassen CD. Quantitative-profiling of bile acids and their conjugates in mouse liver, bile, plasma, and urine using LC-MS/MS. J Chromatogr B Analyt Technol Biomed Life Sci. 2008;873:209–17.

[14]. Brunt EM, Kleiner DE, Wilson LA, Belt P, Neuschwander-Tetri BA, Network NCR. Nonalcoholic fatty liver disease (NAFLD) activity score and the histopathologic diagnosis

in NAFLD: distinct clinicopathologic meanings. Hepatology. 2011;53:810–20. [PubMed: 21319198]

[15]. Zhang Y, Ge X, Heemstra LA, Chen WD, Xu J, Smith JL, et al. Loss of FXR protects against diet-induced obesity and accelerates liver carcinogenesis in ob/ob mice. Mol Endocrinol. 2012;26:272–80. [PubMed: 22261820]

[16]. Flessa CM, Nasiri-Ansari N, Kyrou I, Leca BM, Lianou M, Chatzigeorgiou A, et al. Genetic and Diet-Induced Animal Models for Non-Alcoholic Fatty Liver Disease (NAFLD) Research. Int J Mol Sci. 2022;23.

[17]. Softic S, Cohen DE, Kahn CR. Role of Dietary Fructose and Hepatic De Novo Lipogenesis in Fatty Liver Disease. Dig Dis Sci. 2016;61:1282–93. [PubMed: 26856717]

[18]. Drury JE, Mindnich R, Penning TM. Characterization of disease-related 5beta-reductase (AKR1D1) mutations reveals their potential to cause bile acid deficiency. J Biol Chem. 2010;285:24529–37. [PubMed: 20522910]

[19]. Lagace TA. PCSK9 and LDLR degradation: regulatory mechanisms in circulation and in cells. Curr Opin Lipidol. 2014;25:387–93. [PubMed: 25110901]

[20]. Wei E, Ben Ali Y, Lyon J, Wang H, Nelson R, Dolinsky VW, et al. Loss of TGH/Ces3 in mice decreases blood lipids, improves glucose tolerance, and increases energy expenditure. Cell Metab. 2010;11:183–93. [PubMed: 20197051]

[21]. Ko KW, Erickson B, Lehner R. Es-x/Ces1 prevents triacylglycerol accumulation in McArdle-RH7777 hepatocytes. Biochim Biophys Acta. 2009;1791:1133–43. [PubMed: 19651238]

[22]. Li Y, Zalzala M, Jadhav K, Xu Y, Kasumov T, Yin L, et al. Carboxylesterase 2 prevents liver steatosis by modulating lipolysis, endoplasmic reticulum stress, and lipogenesis and is regulated by hepatocyte nuclear factor 4 alpha in mice. Hepatology. 2016;63:1860–74. [PubMed: 26806650]

[23]. Pan X, Zhang Y. Hepatocyte nuclear factor 4alpha in the pathogenesis of non-alcoholic fatty liver disease. Chin Med J (Engl). 2022;135:1172–81. [PubMed: 35191422]

[24]. Puche JE, Saiman Y, Friedman SL. Hepatic stellate cells and liver fibrosis. Compr Physiol. 2013;3:1473–92. [PubMed: 24265236]

[25]. Leclere PS, Rousseau D, Patouraux S, Guerin S, Bonnafous S, Grechez-Cassiau A, et al. MCD diet-induced steatohepatitis generates a diurnal rhythm of associated biomarkers and worsens liver injury in Klf10 deficient mice. Sci Rep. 2020;10:12139. [PubMed: 32699233]

[26]. Lee J, Oh AR, Lee HY, Moon YA, Lee HJ, Cha JY. Deletion of KLF10 Leads to Stress-Induced Liver Fibrosis upon High Sucrose Feeding. Int J Mol Sci. 2020;22.

[27]. Yang S, Jia L, Xiang J, Yang G, Qiu S, Kang L, et al. KLF10 promotes nonalcoholic steatohepatitis progression through transcriptional activation of zDHHC7. EMBO Rep. 2022;23:e54229. [PubMed: 35492028]

[28]. Parthasarathy G, Revelo X, Malhi H. Pathogenesis of Nonalcoholic Steatohepatitis: An Overview. Hepatol Commun. 2020;4:478–92. [PubMed: 32258944]

[29]. Malhi H, Gores GJ. Molecular mechanisms of lipotoxicity in nonalcoholic fatty liver disease. Semin Liver Dis. 2008;28:360–9. [PubMed: 18956292]

[30]. Xu Y, Zalzala M, Xu J, Li Y, Yin L, Zhang Y. A metabolic stress-inducible miR-34a-HNF4alpha pathway regulates lipid and lipoprotein metabolism. Nat Commun. 2015;6:7466. [PubMed: 26100857]

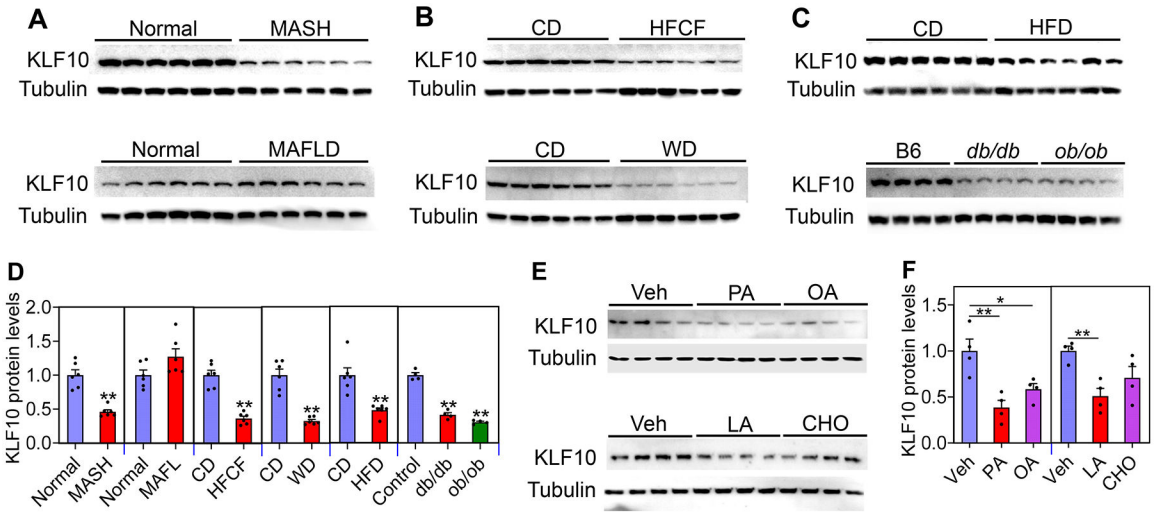

Figure 1. Hepatic KLF10 expression is reduced in MASLD patients and diet-induced or genetically obese mice.

(A) Western blot assays of proteins isolated from MASH (top panel) or MAFLD (bottom panel) patients and normal individuals (n=6 per group). (**B-C)** Hepatic KLF10 protein levels in mice fed a high-fat/cholesterol/fructose (HFCF) diet (**B**, top panel), Western diet (WD) (**B**, bottom panel) or high-fat diet (HFD) (**C**, top panel) for 16 weeks (n=6 per group), or in *db/db* or *ob/ob* mice (**C**, bottom panel) (n=4 per group). CD, chow diet. B6, C57BL/6J mice. **(D)** Quantitative protein levels for studies described in **A-C**. **(E-F)** Primary hepatocytes were treated with bovine serum albumin (BSA; Veh), 100 μM palmitic acid (PA), oleic acid (OA), or linoleic acid (LA) or 10 μg/ml cholesterol (CHO) for 48 hours. Western blot assays were performed (**E**) and protein levels were quantified (**F**) (n=4 per group). Data are expressed as mean±SEM. Statistical analysis was performed using a 2-tailed, unpaired *t*-test (**D**) or one-way ANOVA (**D** (*db/db* or *ob/ob* mice), **F**). **P*<0.05, ***P*<0.01

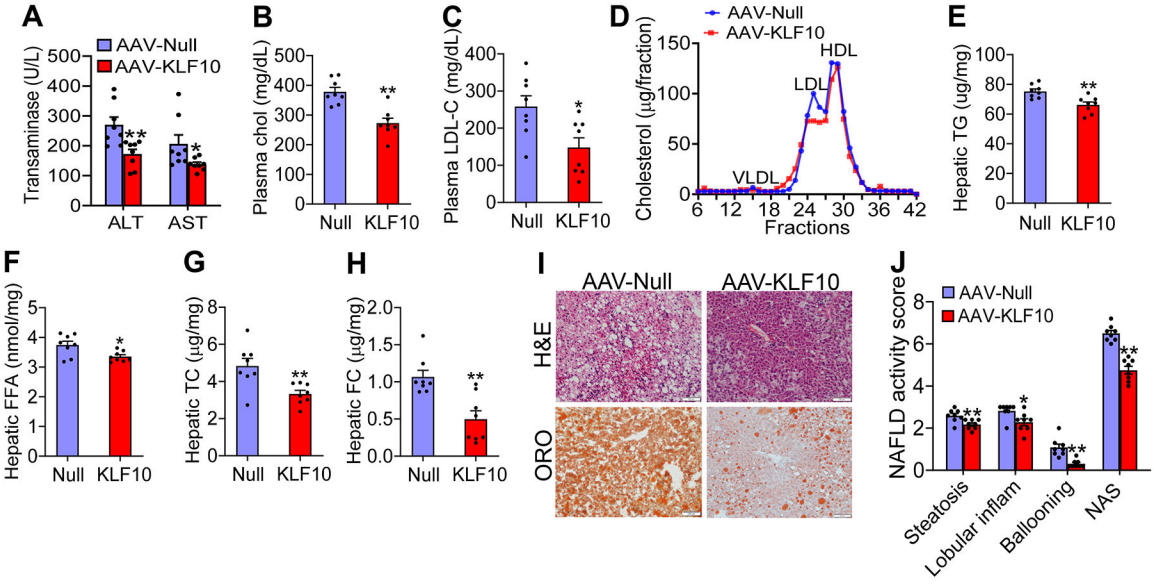

Figure 2. Overexpression of human KLF10 in hepatocytes ameliorates Western diet-induced steatohepatitis and hypercholesterolemia

C57BL/6 mice were i.v. injected with AAV8-ALB-Null or AAV8-ALB-hKLF10, then fed a Western diet for 16 weeks (n=8 per group). **(A)** Plasma ALT and AST levels. **(B)** Plasma total cholesterol (TC) levels. Chol, cholesterol. **(C)** Plasma low-density lipoprotein (LDL) cholesterol (LDL-C) levels. **(D)** Plasma cholesterol lipoprotein profile was analyzed by fast protein liquid chromatography (FPLC). **(E)** Hepatic triglyceride (TG) levels. **(F)** Hepatic free fatty acid (FFA) levels. **(G)** Hepatic total cholesterol (TC) levels. **(H)** Hepatic free cholesterol (FC) levels. **(I)** Liver sections were stained with H&E or Oil red O. **(J)** NAFLD activity (NAS) was determined after histological grading of steatosis, lobular inflammation, and hepatocyte ballooning. Scale bars in **I**: 100 μm. Data are expressed as mean±SEM. Statistical analysis was performed using a 2-tailed, unpaired *t*-test (**A-C, E-H, J**). **P*<0.05, ***P*<0.01

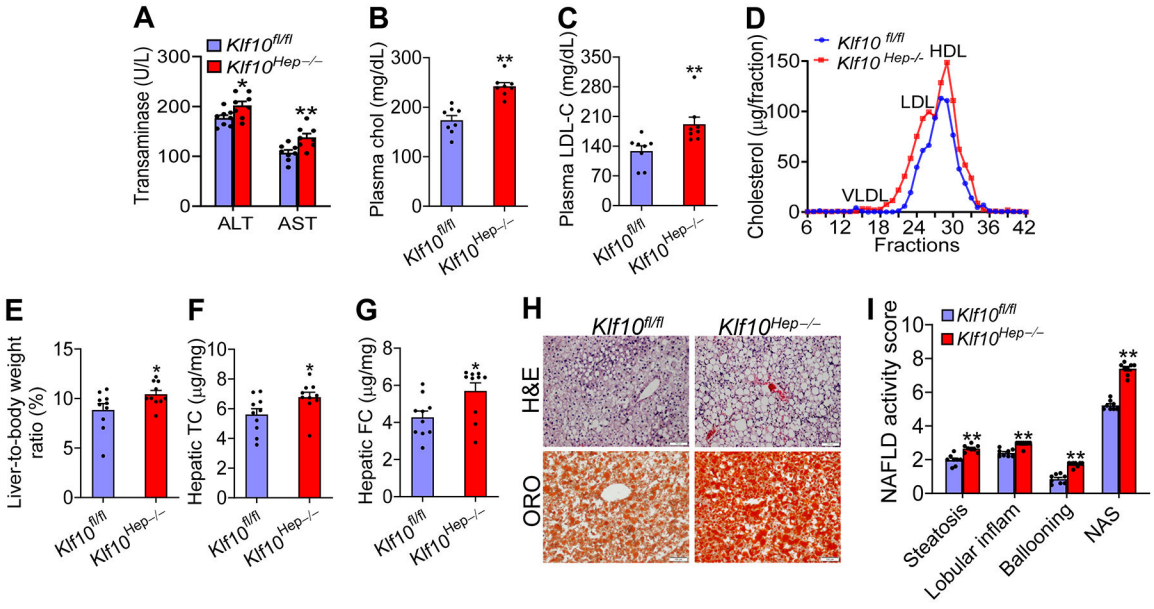

Figure 3. Ablation of hepatocyte KLF10 aggravates Western diet-induced steatohepatitis and hypercholesterolemia

Klf10$^{fl/fl}$ mice and *Klf10*$^{Hep-/-}$ mice were fed a western diet for 16 weeks (n=8 per group). **(A)** Plasma transaminase levels. **(B)** Plasma total cholesterol levels. **(C)** Plasma LDL-C levels. **(D)** Plasma cholesterol lipoprotein profiles. **(E)** Liver-to-body weight ratio. **(F)** Hepatic total cholesterol (TC) levels. **(G)** Hepatic free cholesterol (FC) levels. **(H)** H&E or Oil red O staining of liver sections. Scale bars in **H**: 100 μm. Data are expressed as mean±SEM. Statistical analysis was performed using a 2-tailed, unpaired *t*-test (**A-C, E-G, I**). **P*<0.05, ***P*<0.01

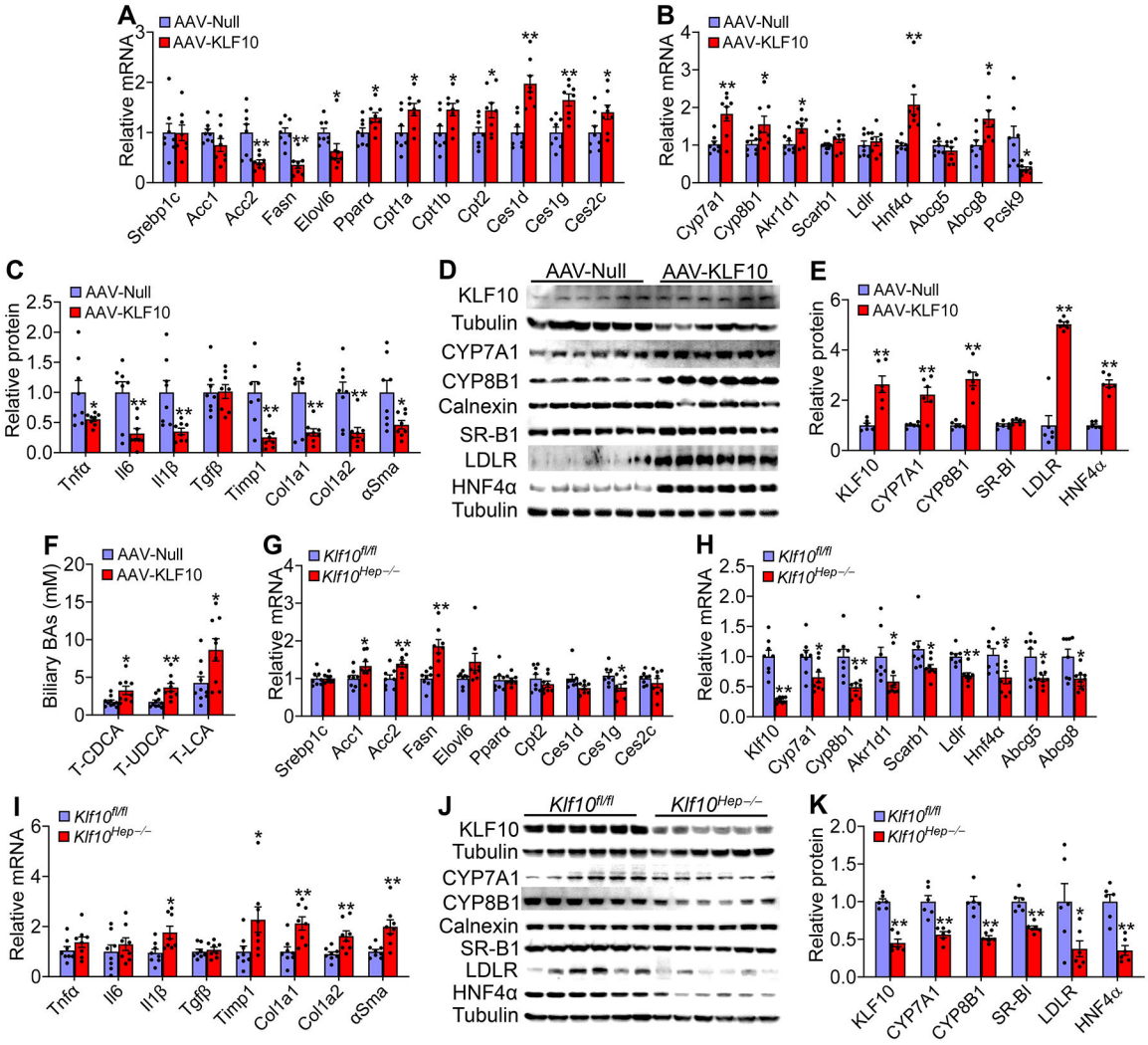

Figure 4. Hepatocyte KLF10 regulates genes involved in triglyceride and cholesterol metabolism and inflammation

(A-F) C57BL/6 mice were i.v. injected with AAV8-ALB-Null or AAV8-ALB-hKLF10, then fed a western diet for 16 weeks (n=8 per group). Hepatic mRNA levels (**A-C**) and protein levels (**D-E**) were determined. Bile acid composition in bile was determined (**F**). **(G-K)** *Klf10*$^{fl/fl}$ mice and *Klf10*$^{Hep-/-}$ mice were fed a Western diet for 16 weeks (n=8 per group). Hepatic mRNA levels (**G-I**) and protein levels (**J-K**) were determined. Data are expressed as mean±SEM. Statistical analysis was performed using a 2-tailed, unpaired *t*-test (**A-C, E-I, K**). **P*<0.05, ***P*<0.01

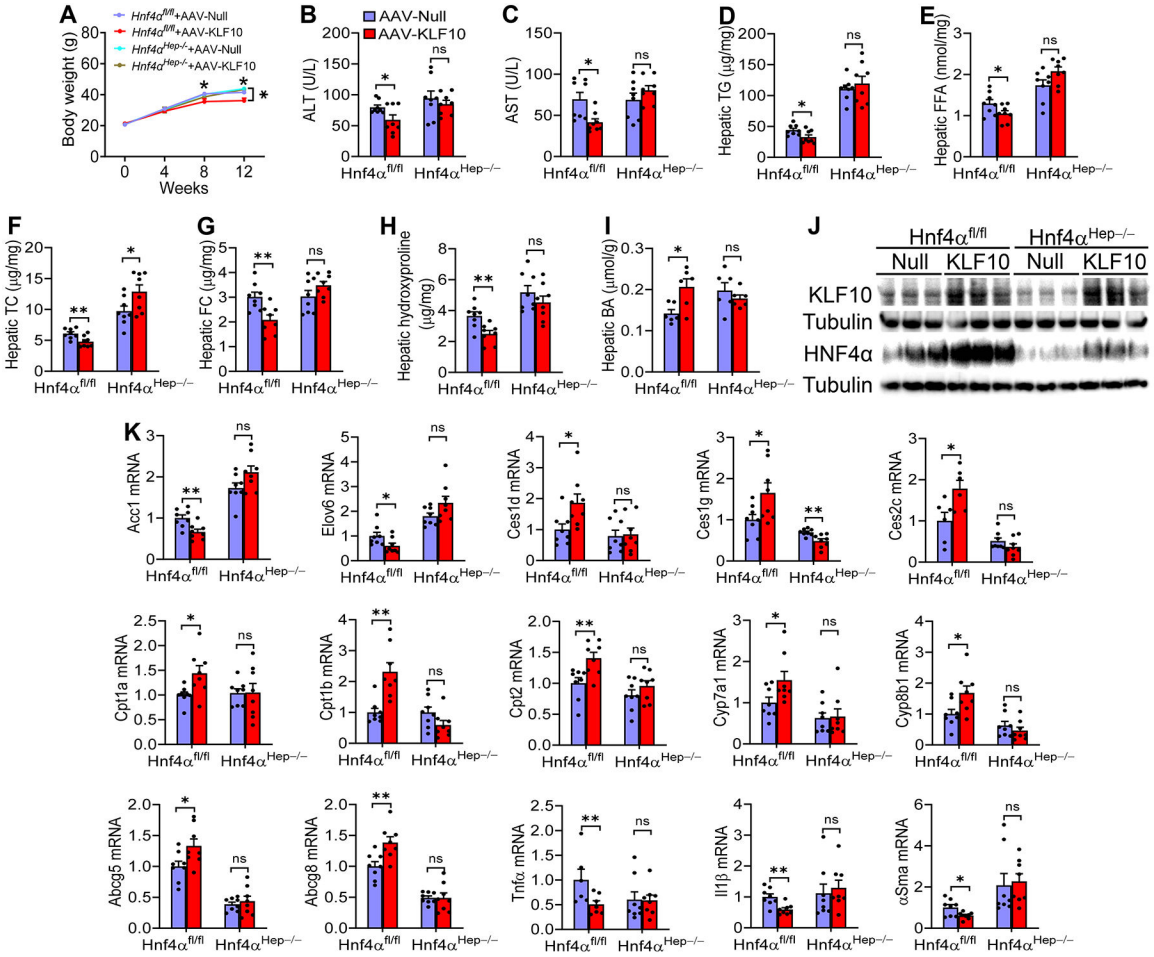

Figure 5. Hepatocyte KLF10 prevents MASH development via HNF4α

Hnf4α$^{fl/fl}$ mice and *Hnf4α*$^{Hep-/-}$ mice were i.v. injected with AAV8-ALB-Null or AAV8-ALB-hKLF10, then fed a Western diet (WD) (n=8 per group) for 12 weeks. **(A)** Body weight. **(B)** Plasma ALT levels. **(C)** Plasma AST levels. **(D)** Hepatic triglyceride (TG) levels. **(E)** Hepatic free fat acid (FFA) levels. **(F)** Hepatic total cholesterol (TC) levels. **(G)** Hepatic free cholesterol (FC) levels. **(H)** Hepatic hydroxyproline levels. **(I)** Hepatic bile acid (BA) levels. **(J)** Hepatic protein levels. **(K)** Hepatic mRNA levels. Data are expressed as mean±SEM. Statistical analysis was performed using two-way ANOVA (**A-I, K**). ns, not significant. **P*<0.05, ***P*<0.01

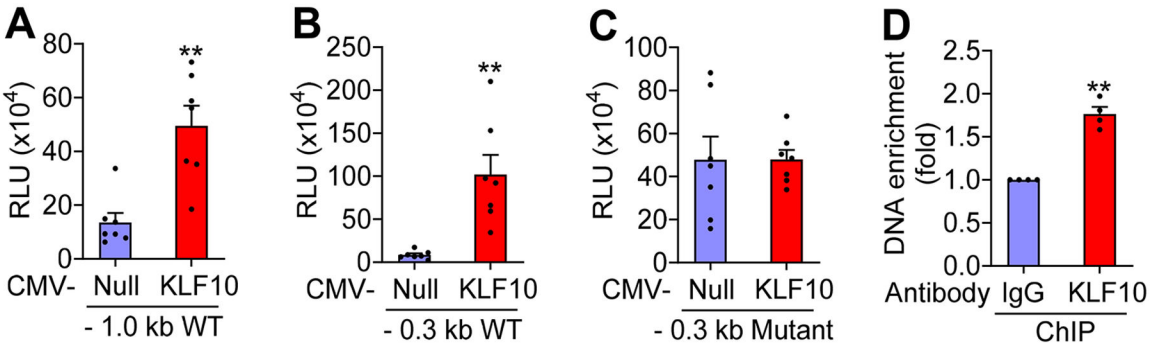

Figure 6. HNF4α is a direct target gene of KLF10

(A-C) Transient transfections were performed by co-transfecting CMV-Null or CMV-KLF10 with pGL3-HNF4α (−1.0 kb WT) (**A**), pGL3- HNF4α (−0.3 kb WT) (**B**) or pGL3- HNF4α (−0.3 kb Mutant) (**C**) into HepG2 cells (n=7). After 24 h, relative luciferase activities (RLU) were determined after normalizing to beta-galactosidase activity. WT, wild-type. **(D)** C57BL/6 mice were i.v. injected with AAV8-ALB-Null or AAV8-ALB-hKLF10, then fed a Western diet for 16 weeks. ChIP assays were performed using liver lysates overexpressing KLF10 and IgG (control) or the KLF10 antibody (n=3). The DNA enrichment in the *Hnf4α* promoter was determined by qRT-PCR using primers that amplified a fragment between −227 bp and −154 bp (**D**). Statistical analysis was performed using a 2-tailed, unpaired *t*-test (**A-D**). ** $P<0.01$

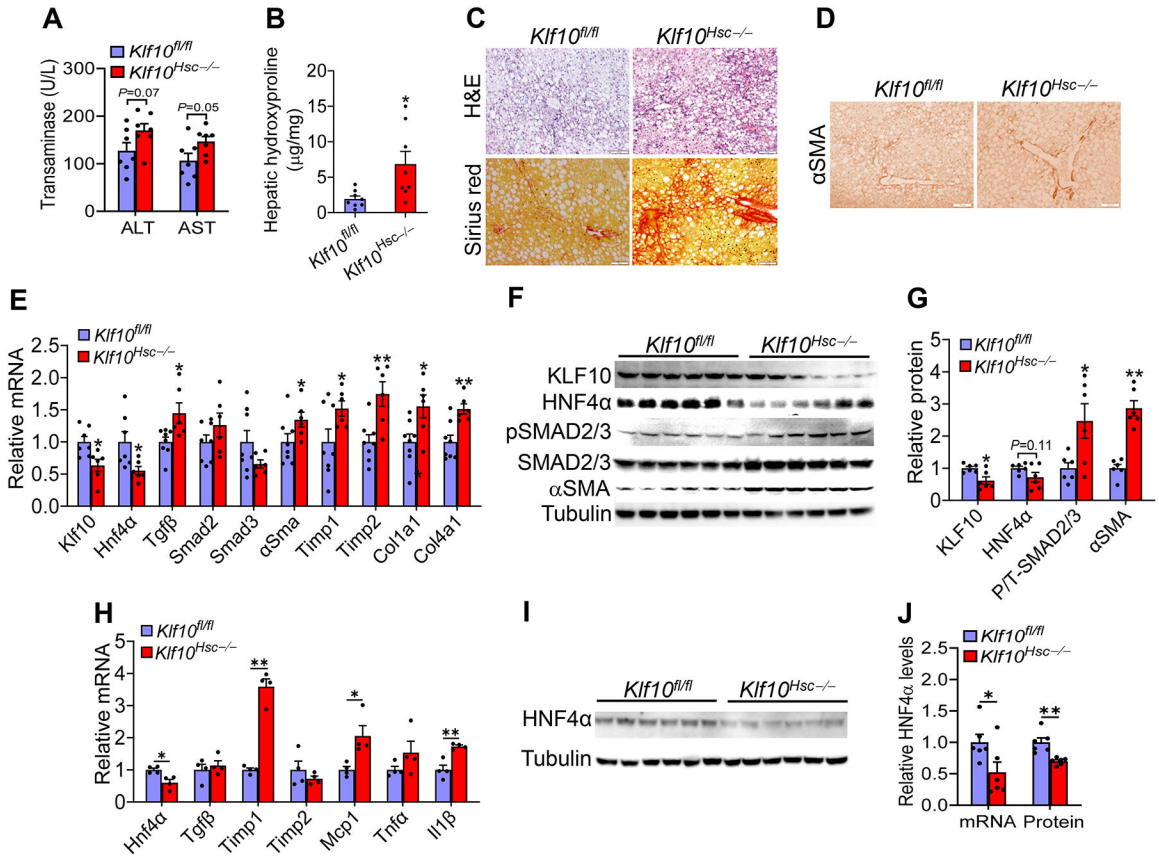

Figure 7. Ablation of KLF10 in hepatic stellate cells aggravates HFCF diet-induced fibrogenesis

(**A-G**) *Klf10*$^{fl/fl}$ mice and *Klf10*$^{HSC-/-}$ mice were fed a HFCF diet for 20 weeks (n=7 per group). **(A)** Plasma transaminase levels. **(B)** Hepatic hydroxyproline levels. **(C)** Liver sections were stained by H&E or picrosirius red. **(D)** Immunohistochemical staining of liver staining using an αSMA antibody. **(E)** Hepatic mRNA levels. **(F-G)** Hepatic protein levels. Scale bars in **C-D**: 100 μm. **(H)** HSC were isolated from *Klf10*$^{fl/fl}$ mice and *Klf10*$^{HSC-/-}$ mice and then cultured for 48 h. The conditioned media were used to treat primary hepatocytes isolated from C57BL/6 mice. After 24 h, mRNA levels were quantified (n=4). **(I-J)** Primary hepatocytes were isolated from *Klf10*$^{fl/fl}$ mice and *Klf10*$^{HSC-/-}$ mice. After 6 h, *Hnf4α* mRNA and protein levels were quantified (n=6). Data are expressed as mean±SEM. Statistical analysis was performed using a 2-tailed, unpaired *t*-test (**A-B, E, G, H, J**). **P*<0.05, ***P*<0.01